Impact of the ^{87}Rb singlet scattering length on suppressing inelastic collisions

James P. Burke, Jr.,[1] John L. Bohn,[2] B. D. Esry,[1] and Chris H. Greene[1]
[1]*JILA and the Department of Physics, University of Colorado, Boulder, Colorado 80309-0440*
[2]*Quantum Physics Division, NIST, Boulder, Colorado 80309*
(Received 14 November 1996)

A computation of ^{87}Rb-^{87}Rb spin-exchange rate constants as functions of the two-body singlet scattering length a_s demonstrates that the inelastic collision rate is suppressed over a small range of the possible values for a_s. A two-channel model relates this inelastic suppression to an interference phenomenon, manifested in the near coincidence of the singlet and triplet scattering lengths. This mechanism explains the diminished rates measured in recent ''double-trap'' experiments. Combining information extracted from these rates and from previous scattering length measurements allows us to place bounds on the ^{87}Rb singlet scattering length (74–102 a.u.). [S1050-2947(97)50104-1]

PACS number(s): 03.80.+r, 32.80.Pj, 05.30.Jp

Recently Myatt *et al.* [1] succeeded in trapping simultaneously two distinct species of ^{87}Rb atoms in a magnetic trap. These species, distinguished by their total spin quantum numbers $|fm_f\rangle = |2,2\rangle$ and $|1,-1\rangle$, had been previously trapped individually, but were expected to suffer large inelastic collision rates when placed in the same trap, leading to the rapid destruction of a cloud containing both species. Nevertheless, Ref. [1]'s experiment successfully trapped both species in overlapping clouds and even attained simultaneous Bose-Einstein condensation (BEC) of both species by evaporatively cooling only the $|1,-1\rangle$ state; the $|2,2\rangle$ state cooled ''sympathetically,'' i.e., only through its thermal contact with the $|1,-1\rangle$ state. This remarkable result demonstrates a dramatic dominance of elastic over inelastic processes in collisions between the two species. It also raises the intriguing possibility that sympathetic cooling could be used to produce BEC in atomic species that are not naturally conducive to evaporative cooling techniques, or as a means of producing degenerate gases of fermionic atoms.

Previous theoretical estimates had failed to appreciate the suppression of inelastic relative to elastic scattering as they were hampered by large uncertainties in the singlet scattering length of two rubidium atoms. We therefore compute in this Rapid Communication *s*-wave spin-exchange relaxation rates as functions of the singlet scattering length. Our results show a drastic suppression of the inelastic rates when the scattering length a_s for singlet electronic states *nearly coincides* with the scattering length a_t for triplet electronic states. The combination of our theoretical study with the measurement of unexpectedly low inelastic rates by Myatt *et al.* [1] then demonstrates that these scattering lengths must in fact nearly coincide for ^{87}Rb. This circumstance allows us (along with Julienne *et al.* [2], who also noted the suppression mechanism) to put relatively narrow bounds on a_s. These bounds also restrict scattering lengths for collisions between the two atomic species, with important implications for condensates containing atoms in both spin states, as we have reported recently [3].

The collisional dynamics of two alkali atoms possesses different sets of approximately good quantum numbers in small and large regions of internuclear distance R, separated by an ''interaction'' region that occurs at roughly $R_I \sim 20-25$ a.u. in ^{87}Rb. In the small R region ($R<R_I$), the collision is best represented in a molecular basis of total electron (S) and nuclear (I) spin $|Sm_s\rangle|Im_I\rangle$, and characterized by Born-Oppenheimer molecular singlet ($S=0$) and triplet ($S=1$) potentials that dominate the weak hyperfine interactions. Asymptotically ($R>R_I$), the hyperfine interactions instead dominate over the exponentially decaying exchange splitting between singlet and triplet channels; an atomic basis of total spin $|f_a m_{f_a}\rangle|f_b m_{f_b}\rangle$, which diagonalizes the hyperfine interaction, becomes most appropriate. Here $\vec{f}_a = \vec{s}_a + \vec{i}_a$ and a and b label the two atoms. At intermediate R ($R \sim R_I$), the hyperfine and exchange energies compete, driving ''spin exchange'' processes that can scatter atoms into untrapped spin states or else impart sufficient energy to eject atoms from the trap.

In our analysis, we focus on the following incident channels ($|f,m_f\rangle$): (a) $|2,2\rangle + |1,-1\rangle$; (b) $|2,1\rangle + |1,-1\rangle$; (c) $|2,1\rangle + |2,1\rangle$. The first represents the dominant interspecies collisions, whose inelastic rate must be low for the sympathetic cooling in the Myatt *et al.* experiment to be effective. Collisions involving the $|2,1\rangle$ state are relevant for explaining the small ($\sim 1\%$) observed amount of this species in the experiment. In addition, these collisions will serve below to illustrate that the inelastic suppression mechanism is independent of which hyperfine states collide. Our full close-coupling calculations therefore include all the incident channels (a)–(c), along with their accessible *s*-wave product channels.

Other permutations of colliding species relax only through second-order processes, and are therefore neglected in our analysis. For example, a collision between two $|2,2\rangle$ ''stretched-state'' atoms (all spins aligned) projects only onto a triplet Born-Oppenheimer state, rendering spin exchange impossible. A collision of this type can relax only through second-order processes such as dipolar spin relaxation, whose inelastic rate constant has been measured to be no greater than 5×10^{-15} cm^3/sec [4] and is predicted to be much smaller ($0.4–2.4\times10^{-15}$ cm^3/sec) [5]. Similarly, conservation of parity prohibits spin exchange in a $|2,2\rangle + |2,1\rangle$ *s*-wave collision. A $|2,2\rangle + |2,1\rangle$ *p*-wave collision will suffer

from spin exchange but again should be suppressed according to the Wigner threshold law and is thus irrelevant at μK trap temperatures.

We use as triplet and singlet Born-Oppenheimer potentials the highly accurate *ab initio* pseudopotentials of Krauss and Stevens [6] for $R<20$ a.u., joined onto the long-range dispersion potential of Marinescu, Sadeghpour, and Dalgarno [7] and the long-range exchange potentials of Smirnov and Chibisov [8] for $R>20$ a.u. The singlet scattering length was varied by adjusting the coefficient of a quadratic addition to the inner wall of the singlet potential in the manner of Mies *et al.*, who justify this procedure in detail [5]. We solved the coupled multichannel radial Schrödinger equations using a finite-element (FEM) [9] R-matrix [10] approach. We calculate the R matrix at a large radius R_0, beyond which we can neglect long-range atomic interactions. Matching the wave functions and their derivatives at the boundary R_0 to spherical Bessel functions leads to a scattering matrix $\underline{S}$ [11] and transition matrix $\underline{T}=i(\underline{S}-\underline{1})$ [12]. The rate coefficient κ_{ij} for an atom pair incident in channel j to exit in channel i is given by

$$\kappa_{ij}=\frac{\pi\hbar}{\mu k_j}|T_{i,j}|^2 \tag{1}$$

where μ is the reduced mass of Rb_2 and k_j is the wave number in the entrance channel. The inelastic rate coefficient κ_{ij} $(i\neq j)$ represents an event rate with the loss of two atoms in any exit channel consisting of two untrapped states. The total inelastic event rate coefficients quoted below must therefore be multiplied by two to yield individual atom loss rates.

The total event rate coefficients for the three incident channels listed above are shown in Fig. 1 versus an assumed singlet scattering length a_s, with the triplet scattering length a_t held constant at the nominal measured value [14] of 110 a.u. The scattering energy is taken as 1 μK; calculations at other energies verify that our results obey the Wigner threshold laws. Figure 1 shows features distinctive to all three collisions: (i) The elastic rate constant is roughly independent of the singlet scattering length and of the same order of magnitude for all processes ($\sim 10^{-11}$ cm^3/sec). (ii) The inelastic rate constant drops by several orders of magnitude over a relatively small range of singlet scattering lengths near $a_s=100$ a.u. Since successful sympathetic cooling requires hundreds of elastic collisions per inelastic event, the results plotted in Fig. 1 along with the production of BEC in the Myatt *et al.* experiment immediately imply that a_s must lie near 100 a.u.

We interpret this strong suppression of inelastic rates in the spirit of generalized multichannel quantum-defect theory [11]. Physically, there are many channels accessible to the collision complex, but at short range $R<R_I$ the multichannel set consists of approximately uncoupled degenerate channels that project onto either the singlet or triplet molecular states. We therefore consider only the uncoupled singlet and triplet molecular potentials, writing the corresponding short range scattering matrix $\underline{S}$ as

$$\underline{S}=\begin{pmatrix} e^{2i\delta_s} & 0 \\ 0 & e^{2i\delta_t} \end{pmatrix}, \tag{2}$$

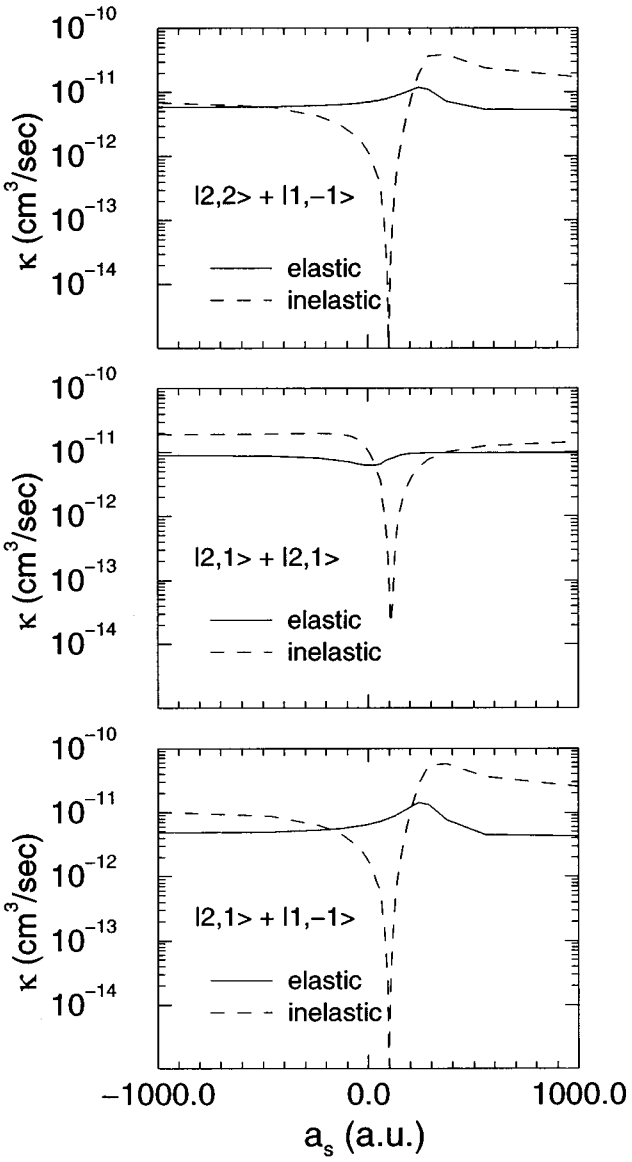

FIG. 1. ^{87}Rb elastic and total inelastic rate constants κ as functions of an assumed singlet scattering length a_s. The entrance channel is noted on each figure panel. Rate constants were calculated for an incident energy of 1 μK above threshold and a constant triplet scattering length of 110 a.u.

where $\delta_{s/t}$ is the phase shift in the singlet or triplet channel. For a given incident channel and a single exit channel, the influence of hyperfine coupling can be parametrized in terms of a mixing angle θ [12] that rearranges the scattering matrix $\underline{S}'$ into

$$S'=\begin{pmatrix} \cos^2\theta e^{2i\delta_s}+\sin^2\theta e^{2i\delta_t} & \frac{1}{2}\sin 2\theta(e^{2i\delta_s}-e^{2i\delta_t}) \\ \frac{1}{2}\sin 2\theta(e^{2i\delta_s}-e^{2i\delta_t}) & \cos^2\theta e^{2i\delta_t}+\sin^2\theta e^{2i\delta_s} \end{pmatrix}.$$

The squared off-diagonal elements of the new scattering matrix $\underline{S}'$ relevant to inelastic scattering are proportional to $\sin^2 2\theta \sin^2(\delta_s-\delta_t)$, so that regardless of the hyperfine mixing, complete inelastic suppression occurs when the accumulated phase shifts in the singlet and triplet channels are equal in the interaction region R_I. (The singlet and triplet eigen-

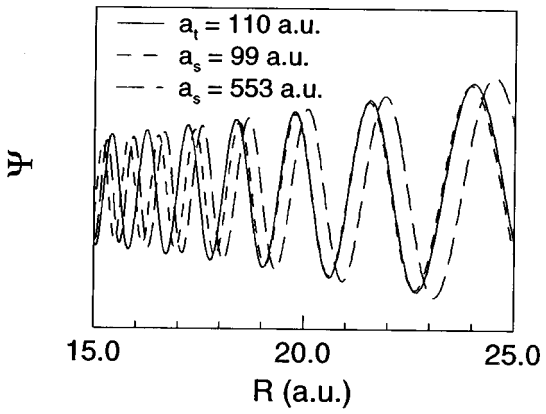

FIG. 2. Zero-energy single-channel wave functions for the singlet and triplet (solid line) molecular potentials as functions of the internuclear distance R.

phase shifts at $R\rightarrow\infty$ also remain approximately equal, because the molecular potentials quickly become degenerate for $R>R_I$.) We can therefore relate inelastic suppression to the coincidence of the singlet and triplet scattering lengths. A similiar interpretation emerges from the analysis of Dalgarno and Rudge [13].

Zero-energy singlet and triplet wave functions are shown in Fig. 2. We see in the region of maximum coupling (20 a.u. $<R<$25 a.u.) that the singlet wave function with a scattering length $a_s=99$ a.u. is nearly in phase with the triplet, while that with $a_s=553$ a.u. is out of phase. Changing the singlet potential to allow a_s to vary from $-\infty$ to $+\infty$ introduces one additional node into the singlet wave function, pushing it through a π phase change in the interaction region R_I. The result is one region of inelastic suppression per a_s cycle.

Physically, the incoming incident wave splits when it propagates inward through the interaction region (R_I), sending amplitude into both singlet and triplet channels at short range. These wave components evolve nearly independently, reflect from their inner turning points, then recombine in the interaction region to produce the final mixture of exit channels. If the components meet in phase, as in the $a_s=99$ a.u. case, the outgoing waves recombine constructively, reproducing the original channel, in which case the scattering is primarily elastic. Otherwise, the amplitudes recombine destructively, requiring scattering flux to exit in other channels.

The Myatt *et al.* experiment has provided a unique opportunity to estimate the ^{87}Rb singlet scattering length. According to Fig. 1, the empirically determined loss rates limit the permissible range of the singlet scattering length a_s for a given value of a_t. An estimate of the full range of a_s must also account for the ($\pm$10 a.u.) uncertainty of the nominal triplet scattering length $a_t=110$ a.u. [14]. In Fig. 3(a), we plot the loss rates for $|2,2\rangle+|1,-1\rangle$ collisions versus a_s for three different values of a_t (100, 110, and 120 a.u.). The experimentally measured value for the rate constant is included on this graph with error bars. This graph demonstrates that the experimentally measured rate constant already restricts a_s to a fairly narrow range.

In fact, an independently measured value of the scattering length $a_{1,-1}$ for $|1,-1\rangle+|1,-1\rangle$ elastic scattering [15] restricts the range of a_s much more tightly. We calculate

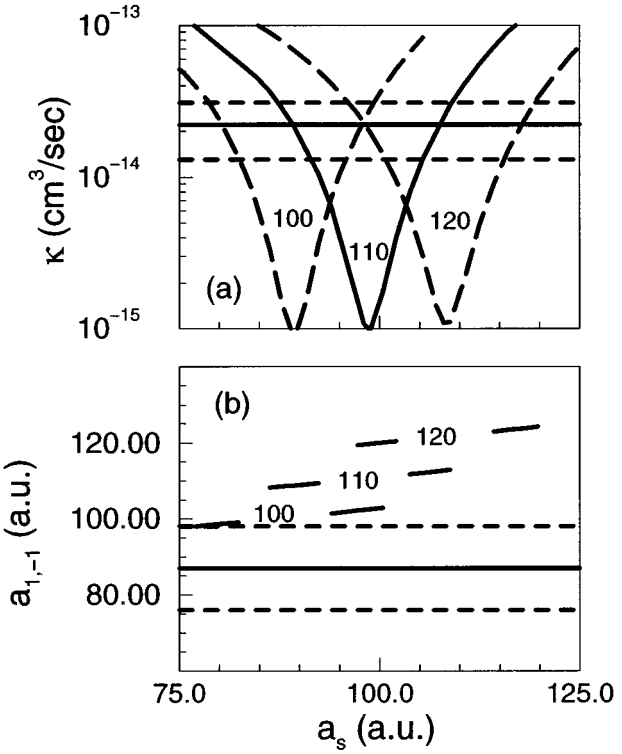

FIG. 3. (a) ^{87}Rb inelastic rate constants κ as functions of an assumed singlet scattering length a_s for a $|2,2\rangle+|1,-1\rangle$ collision. Each curve is calculated with a constant triplet scattering length a_t (100, 110, and 120 a.u.) for an incident energy of 1 μK above threshold. The horizontal lines indicate the mean (solid line) and 1σ uncertainties (dashed line) of the measured value. (b) Calculated scattering length $a_{1,-1}$ for a collision between two $|1,-1\rangle$ atoms versus an assumed singlet scattering length a_s. Each line is calculated using a constant triplet scattering length a_t over a range of a_s values consistent with the measured inelastic rate constant [see (a)]. The horizontal lines indicate the mean (solid line) and 1σ uncertainties (dashed line) of the measured $a_{1,-1}$.

$a_{1,-1}$ for each (a_s,a_t) pair by writing the appropriate diagonal element of the $\underline{S}$ matrix with a complex phase shift $\delta_{1,-1}=-k(a_{1,-1}-ib_{1,-1})$. Figure 3(b) shows the calculated $a_{1,-1}$ scattering length for the three values of a_t shown in Fig. 3(a), over the range of a_s consistent with the Myatt *et al.* experiment. Note that there are two separate ranges of a_s for each value of a_t consistent with the measured $|2,2\rangle+|1,-1\rangle$ inelastic rate constant [see Fig. 3(a)]. Figure 3(b), which includes the measured value of $a_{1,-1}$ with error bars, shows a small region of common overlap, indicating that our calculations based on the double-trap experiment and the a_t mea-

TABLE I. Elastic and inelastic s-wave spin exchange rate constants, in units of cm^3/sec, calculated for an incident energy of 1 μK above threshold. The mean value was calculated using $a_s=81$ a.u. and $a_t=100$ a.u. The error was estimated by varying a_t over the range 93–107 a.u. and a_s over the range 74-102 a.u.

Entrance channel	Elastic rate	Inelastic rate
$\|2,2\rangle+\|1,-1\rangle$	$(6.6\pm0.9)\times10^{-12}$	$(2.3\pm1.1)\times10^{-14}$
$\|2,1\rangle+\|1,-1\rangle$	$(6.5\pm0.9)\times10^{-12}$	$(2.8\pm1.3)\times10^{-14}$
$\|2,1\rangle+\|2,1\rangle$	$(6.3\pm0.9)\times10^{-12}$	$(0.2\text{-}5.0)\times10^{-13}$

surement are consistent with this additional experimental measurement. Our calculations, coupled to an elementary error analysis, translate the uncertainties in the measured values of a_t, $\kappa_{22,1-1}$, and $a_{1,-1}$ into a most probable value for $a_t=100(7)$ a.u. and a range for a_s (74–102 a.u.). In Table I we provide best estimates of the elastic and inelastic rate constants for the three collisional processes shown in Fig. 1. We have solved the appropriate rate equations using these rates, finding trap lifetimes consistent with measured lifetimes. These simulations also generate a population of $|2,1\rangle$ atoms equivalent to $\sim$1% of the total atomic population, which is also consistent with observations.

This near coincidence of a_s and a_t appears fortuitous in ^{87}Rb. In other alkali atoms, such as ^{7}Li and ^{23}Na, this coincidence appears not to be the case [16,17], thus ruling out sympathetic cooling of the type discovered in [1]. However, recent proposals have suggested altering scattering lengths by applying external fields [18]. If these proposals prove feasible, sympathetic cooling could become a viable tool for producing degenerate Fermi gases or BEC in alkali atoms for which other methods have not been successful.

Note added: Recently, it has come to our attention that another group has investigated the suppression of inelastic collisions [19].

We would like to thank Carl Williams for his assistance and acknowledge our many useful discussions with the JILA BEC collaboration. This work was supported in part by the National Science Foundation; J.L.B. acknowledges support from the National Research Council.

[1] C. J. Myatt, E. A. Burt, R. W. Ghrist, E. A. Cornell, C. E. Wieman, Phys. Rev. Lett. **78**, 586 (1997).
[2] P. S. Julienne, F. H. Mies, E. Tiesinga, and C. J. Williams (unpublished).
[3] B. D. Esry, C. H. Greene, J. P. Burke, Jr., and J. L. Bohn (unpublished).
[4] C. J. Myatt (private communication).
[5] F. H. Mies, C. J. Williams, P. S. Julienne, M. K. Krauss, J. Res. Natl. Inst. Stand. Technol. **101**, 521 (1996).
[6] M. Krauss and W. J. Stevens, J. Chem. Phys. **93**, 4236 (1990).
[7] M. Marinescu, H. R. Sadeghpour, and A. Dalgarno, Phys. Rev. A **49**, 982 (1994).
[8] B. M. Smirnov and M. I. Chibisov, Pis'ma Zh. Eksp. Teor. Fiz. **48**, 939 (1965) [JETP Lett. **21**, 624 (1965)].
[9] J. P. Burke, Jr., C. H. Greene, and B. D. Esry, Phys. Rev. A **54**, 3225 (1996).
[10] C. H. Greene, *Fundamental Processes of Atomic Dynamics* (Plenum, New York, 1988), p. 105; C. H. Greene and L. Kim, Phys. Rev. A **38**, 5953 (1988); H. Le Rouzo and G. Raseev, *ibid.* **29**, 1214 (1984).
[11] M. Aymar, C. H. Greene, E. Luc-Koenig, Rev. Mod. Phys. **68**, 1015 (1996).
[12] N. F. Mott and H. S. W. Massey, *The Theory of Atomic Collisions* (Oxford University Press, Oxford, 1965), p. 371.
[13] A. Dalgarno and M.R.H. Rudge, Proc. R. Soc. London, Ser. A, **286**, 519 (1965).
[14] H. M. J. M. Boesten, C. C. Tsai, J. R. Gardner, D. J. Heinzen, and B. J. Verhaar, Phys. Rev. A **55**, 636 (1997).
[15] N. Newbury, C. Myatt, and C. Wiemann, Phys. Rev. A **51**, R2680 (1995). This reference quotes incorrect 1 σ error bars on $a_{1,-1}$. Figure 3(b) incorporates the correct value quoted in Ref. [1].
[16] A. J. Moerdijk and B. J. Verhaar, Phys. Rev. Lett. **73**, 518 (1994).
[17] E. Tiesinga, C. J. Williams, P. S. Julienne, K. M. Jones, P. D. Lett, and W. D. Phillips, J. Res. Natl. Inst. Stand. Technol. **101**, 505 (1996).
[18] P. O. Fedichev, Yu. Kagan, G. V. Shlyapnikov, and J. T. M. Walraven, Phys. Rev. Lett. **77**, 2913 (1996); E. Tiesinga, B. J. Verhaar, and H. T. C. Stoof, Phys. Rev. A **47**, 4114 (1993); J. L. Bohn and P. S. Julienne (unpublished).
[19] S. J. J. M. F. Kokkelmans, H. M. J. M. Boesten, and B. J. Verhaar (unpublished); J. M. Vogels, C. C. Tsai, R. S. Freeland, S. J. J. M. F. Kokkelmans, B. J. Verhaar, and D. J. Heinzen (unpublished).